Original Paper

Neuro
-endocrinology

Neuroendocrinology
DOI: 10.1159/000500159

Received: November 14, 2018
Accepted after revision: April 4, 2019
Published online: June 13, 2019

The Oncolytic Herpes Simplex Virus Talimogene Laherparepvec Shows Promising Efficacy in Neuroendocrine Cancer Cell Lines

Linus D. Kloker[a] Susanne Berchtold[a, b] Irina Smirnow[a] Martin Schaller[c] Birgit Fehrenbacher[c] Andreas Krieg[d] Bence Sipos[a] Ulrich M. Lauer[a, b]

[a]Department of Clinical Tumor Biology, University Hospital, University of Tübingen, Tübingen, Germany;
[b]German Cancer Consortium (DKTK), German Cancer Research Center (DKFZ), Tübingen, Germany;
[c]Department of Dermatology, University Hospital, University of Tübingen, Tübingen, Germany;
[d]Department of Surgery (A), Heinrich-Heine-University and University Hospital Düsseldorf, Düsseldorf, Germany

Keywords
Oncolytic virotherapy · Talimogene laherparepvec · Neuroendocrine cancer · Immunotherapy

Abstract
Metastatic neuroendocrine cancer still constitutes a palliative situation, lacking promising treatment options. Oncolytic virotherapy, a novel type of virus-based immunotherapy, lyses tumor cells using genetically engineered viruses thereby activating the immune system to induce an optimized antitumor response which could bring down tumor masses to a stage of minimal residual tumor disease. The oncolytic vector talimogene laherparepvec (T-VEC, herpes simplex virus [HSV] type 1) has already shown excellent safety profiles in clinical studies and has become the first ever FDA/EMA-approved oncolytic virus (OV). This work presents a first preclinical assessment of this state-of-the-art OV, using a panel of human neuroendocrine tumor/neuroendocrine carcinoma (NET/NEC) cell lines. Cytotoxicity, transgene expression, and viral replication patterns were studied. Furthermore, the antiproliferative activity was compared to the one of mTOR inhibitor Everolimus and also interactions between the OV and Everolimus were evaluated. Moreover, virostatic effects of ganciclovir (GCV) on replication of T-VEC were assessed and electron microscopic pictures were taken to comprehend viral envelopment and details of the replication cycle of T-VEC in human neuroendocrine cancer. It could be shown that T-VEC infects, replicates in, and lyses human NET/NEC cells exhibiting high oncolytic efficiencies already at quite low virus concentrations. Interestingly, Everolimus was not found to have any relevant impact on rates of viral replication, but no additive effects could be proved using a combinatorial therapy regimen. On the other hand, GCV was shown to be able to limit replication of T-VEC, thus establishing an important safety feature for future treatments of NET/NEC patients. Taken together, T-VEC opens up a promising novel treatment option for NET/NEC patients, warranting its further preclinical and clinical development.

Introduction

Neuroendocrine tumors (NETs) are a diverse and rare group of tumors, but with rapidly increasing incidence (e.g., as documented in the United States [1]). Due to their generally slow proliferation, NETs are often asymptomatic in early disease stages and hence only diagnosed in a late, metastatic state where no curative therapies are

E-Mail karger@karger.com
www.karger.com/nen

Ulrich M. Lauer
Internal Medicine VIII, Department of Clinical Tumor Biology
University Hospital Tübingen, University of Tübingen
Otfried-Müller-Strasse 10, DE–72076 Tübingen (Germany)
E-Mail ulrich.lauer@uni-tuebingen.de

available any longer. In this situation, the current treatment options include somatostatin analogs, interferon, the mTOR inhibitor Everolimus, the multikinase inhibitor Sunitinib, peptide receptor radiotherapy, radiation, or debulking surgery [2]. For high-grade neuroendocrine carcinomas (NECs), systemic chemotherapy, and radiation are often the only possible choices but associated with a poor prognosis.

Oncolytic virotherapy has already shown its potential in clinical studies with other tumor entities, opening up the opportunity for a complete, durable response [3, 4]. The underlying mechanism of action involves tumor cell selective replication of genetically tumor-targeted viruses, subsequent "direct" tumor cell lysis and the production of viral progeny in tumor cells to amplify the oncolytic process and facilitate an infectious spread within the tumor. The durable, secondary antitumor activity is mediated by the patient's immune system, which gets primed against tumor antigens due to the inflammatory environment created by the combination of tumor cell lysis and massive virus replication [5, 6].

Talimogene laherparepvec (T-VEC), the virotherapeutic agent employed in this study, is the only EMA/FDA-approved oncolytic virus (OV). T-VEC is a genetically modified herpes simplex virus (HSV) type 1 where a viral gene responsible for virulence has been deleted to ensure tumor-specific replication (ICP 34.5) and another gene normally reducing viral immunogenicity (ICP 47) has been deleted as well. Instead, a GM-CSF transgene has been inserted to enhance the stimulation of the immune system [7]. The first clinical trial for this OV was conducted in 2006 [8], and it has been approved in 2015 as a second-line treatment for late-stage melanoma [9]. For melanoma treatment, it is injected intralesionally and leads to a response in injected as well as noninjected lesions, taking the advantage of both direct tumor cell lysis and systemic antitumoral immune activity [10]. The duration of response and response rate were shown to be augmented in combination with checkpoint inhibitors such as anti-PD-1 (programmed death 1) and anti-CTLA-4 (cytotoxic T-lymphocyte-associated antigen 4) antibodies [5, 11]. Therefore, T-VEC is currently studied in several clinical studies for combinatorial treatment regimens to expand approval also for other malignancies. Besides melanoma, T-VEC is under clinical investigation for diverse tumor entities such as liver tumors (NCT02509507), pancreatic cancer (NCT03086642), breast cancer (NCT02658812), or sarcoma (NCT03069378). But, until now, it has not been investigated for its efficacy in neuroendocrine malignancies neither in a clinical nor a preclinical setting.

So far, there are only 2 clinical studies using virotherapeutics to treat neuroendocrine cancer. One phase I trial was conducted with intravenous administration of Seneca Valley virus (SVV-001) for patients with small-cell lung cancer (SCLC) and NETs, but it only showed promising results for SCLC [12]. In another ongoing clinical phase I/II study (NCT02749331), a genetically engineered adenovirus (AdVince) is injected in the hepatic artery to treat NETs exhibiting liver metastases. AdVince has been specifically targeted to NET cells by putting the viral E1A gene, which is crucial for viral replication, under the human chromogranin A promoter [13]. Further virotherapeutic approaches with adenoviruses for NETs are in preclinical testing [14, 15], but no other OVs than SVV-001 and adenoviruses have been evaluated for their efficacy in NETs yet.

Everolimus is an mTOR inhibitor and thus affects the PI3K/Akt/mTOR signaling pathway, which is frequently altered in NETs [16, 17]. It was approved for treatment of progressive advanced lung and intestinal NETs in 2016 and earlier for treatment of progressive advanced pancreatic NETs (pNETs) [18]. Since there is preclinical evidence for synergistic effects of the closely related rapamycin in combination with oncolytic HSVs [19] and other virotherapeutics [20, 21], a combinatorial treatment regimen using Everolimus and virotherapy could be effective for NETs.

Taken together, this paper seeks to verify the antitumor potency of this safe and well-characterized OV against NETs. This is the first study where an oncolytic herpes virus is employed to evaluate if oncolytic virotherapy could be a suitable treatment option for inoperable NETs. For this purpose, viral infection, replication, and tumor cell lysis in human NET/NEC cell lines derived from lung NETs, pNETs and intestinal NECs are assessed. Furthermore, a possible combination of virotherapy with the mTOR inhibitor Everolimus, which is approved for treatment of metastatic gastroenteropancreatic and lung NETs, is evaluated. To prevent safety concerns, the virostatic drug ganciclovir (GCV) is investigated for its potential to attenuate T-VEC activity in NET cells in case of any uncontrollable viral replication features.

Materials and Methods

NET/NEC Cell Lines

A panel of 4 NET and 2 NEC cell lines from different anatomical origins was collected and employed in this study. The 2 pNET cell lines BON-1 and QGP-1 were obtained from Dr. Renner (MPI Psychiatry, Munich, Germany) and the Japanese Collection of Re-

search Bio-Resources Cell Bank, respectively. The H727 and UMC-11 lung NET cell lines both were purchased from ATCC. Moreover, 2 large cell G3 NEC cell lines were employed: HROC-57 cells are derived from a colon ascendens NEC and were obtained from PD Dr. Linnebacher (University Hospital Rostock, Germany). NEC-DUE1 cells descend from a liver metastasis of a pretreated large-cell NEC at gastroesophageal junction and were received from Prof. Krieg (University Hospital Düsseldorf, Germany). All 6 NET/NEC cell lines were characterized and described earlier [22–27]. QGP-1, H727, UMC-1, and NEC-DUE1 cells were maintained in RPMI-1640 medium (Gibco) supplemented with 10% fetal calf serum (FCS, Biochrom). BON-1 cells were cultured in Dulbecco's modified Eagle's Medium (DMEM, Sigma-Aldrich) supplemented with 10% FCS; HROC-57 cells required DMEM/F12 medium (Gibco) with 10% FCS. For virus titrations, Vero cells (African green monkey kidney) were used and obtained from the German Collection of Microorganisms and Cell Cultures (DSMZ, Braunschweig, Germany) and were cultured in DMEM supplemented with 10% FCS.

For treatment or infection cells were seeded in 24-well plates using the following cell counts per well: BON-1 4×10^4, Vero 5×10^4, HROC-57 and H727 6×10^4, UMC-11, and QGP-1 8×10^4, and NEC-DUE1 2×10^5, respectively. Three cell lines were also seeded in 6-well plates using the following cell counts per well: H727 4×10^5, QGP-1 6×10^5, and NEC-DUE1 10^6, respectively. Cells were maintained at 37 °C and 5% CO_2 in a humidified atmosphere.

Everolimus Treatment

Cells were seeded in 24-well plates and treated with Everolimus (Selleckchem) 24 h after seeding. For this purpose, medium was replaced with cell culture medium containing Everolimus in 10-fold dilutions ranging from 10 μM to 10 pM. Cytotoxicity analysis was carried out at 72 and 96 h posttreatment (hpt) with the Sulforhodamine B (SRB) viability assay.

Virus Infection

The OV (T-VEC; HSV type 1 derived) was kindly provided by Amgen Inc., (Thousand Oaks, CA, USA). The virus was stored in aliquots and sonicated in a 4 °C water bath for 30 s immediately after thawing and before usage in cell culture. Cells were seeded in 6- or 24-well plates 24 h prior to infection. T-VEC was diluted in serum-free DMEM to reach the desired multiplicity of infection (MOI; i.e., infectious particles per cultured cell). For infection cells were washed once with phosphate-buffered saline (PBS); then, diluted virus was added. After 1 h of the onset of infection, the inoculum was discarded and replaced with the respective cell culture medium. For mock treatment, the infection medium did not contain any viral particles. For combinatorial treatment, the infection medium was replaced with cell culture medium containing Everolimus at the respective concentration. Cytotoxicity was analyzed at 72 and 96 h postinfection (hpi) with the SRB viability assay.

GCV Treatment

GCV (Selleckchem) was diluted in the respective cell culture medium employing concentrations from 1 to 50 μM and was added at 1 hpi. For addition at 72 hpi, GCV was added to the present cell culture medium.

SRB Viability Assay

Cell viability was measured by the SRB assay [28]. The assay was carried out in 24-well plates, and cell viability was measured compared to mock treatment at 72 and 96 h post Everolimus treatment or post virus infection. Cells were washed with PBS and then fixed with 10% trichloroacetic acid for 30 min at 4 °C. Next, the plate was washed with water and dried in an incubator at 40 °C for 24 h before staining cellular proteins with SRB dye (0.4 in 1% acetic acid, Sigma-Aldrich). After 10 min, unbound dye was removed by washing with 1% acetic acid, the plates were dried overnight, and the SRB dye was dissolved in 10 mM TRIS base (pH 10.5). Absorbance was measured at 550 nm using a Tecan Genios Plus Microplate Reader and was proportional to cell density. The resulting percentage rates refer to the cell number of remaining treated cells compared to the number of mock-treated cells at the same point of time.

Real-Time Cell Monitoring Assay

H727 cells (2×10^4 cells/well) were seeded in 96-well plates (E-Plate 96, Roche Applied Science, Mannheim, Germany). Real-time dynamic cell proliferation was monitored in 30 min intervals during a 120 h observation period using the xCELLigence RTCA SP system (Roche Applied Science). Cell index values were calculated using the RTCA Software (1.0.0.0805). Twenty-four hours after seeding, cells were infected with T-VEC at MOIs 0.001 and 0.0001, respectively, or mock-infected or treated with Everolimus.

Virus Quantification

To create viral growth curves, tumor cells were seeded and infected in 6-well plates. Following infection, plates were washed 3 times with PBS to remove all free viral particles. At the time points 1, 24, 48, 72, and 96 hpi, cells were scraped in the medium, the suspension was harvested and subsequently frozen to induce cell lysis and release of intracellular viral particles. Indicator cells (Vero cells for T-VEC) were seeded in 24-well plates 24 h prior to virus titration. The collected titration samples were thawed quickly, and the indicator cells were infected in duplicates with 10-fold dilutions (10^{-1} to 10^{-6}) of the samples. After 1 h of viral infection with swaying every 15 min, 1.5% carboxymethylcellulose (Sigma-Aldrich) in DMEM with 5% FCS and 1% Pen/Strep were added to prevent viral spread through the culture medium. After 96 h, cells were stained overnight by adding 0.1% crystal violet staining solution (Fluka Chemie AG) (0.1% (w/v) in 5% ethanol, 10% formaldehyde). After washing the plate with tap water, plaques were counted and viral titers (plaque forming units [PFUs] per mL) were determined.

GM-CSF Quantification

H727 and NEC-DUE1 cells were seeded in 6-well plates and infected with T-VEC at MOI 0.0001 (H727) or MOI 0.1 (NEC-DUE1) as described. Supernatants were harvested at the time points 1, 24, 48, 72, and 96 hpi. Analysis of the samples was performed using the LEGEND MAX™ Human GM-CSF ELISA Kit (BioLegend) according to the manufacturer's instructions.

Microscopy

An Olympus IX 50 microscope was employed for microscopic pictures with PhL phase contrast filter. Images were created with the associated F-View Soft Imaging System.

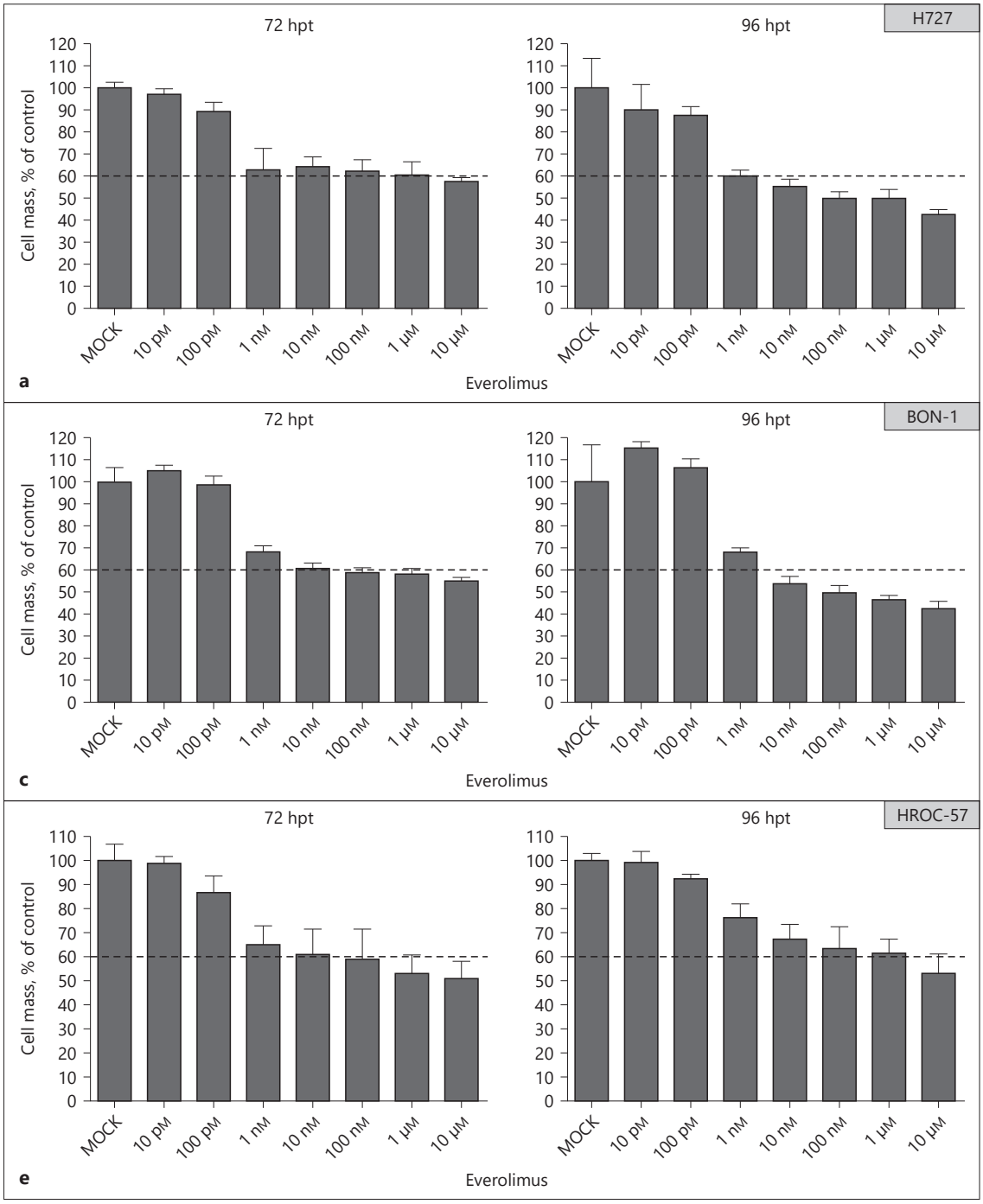

Fig. 1. SRB viability assays employing the clinically approved compound Everolimus on the NET/NEC human cell line panel (analysis performed at 72 and at 96 hpt; mean and SD of 2 independent experiments carried out in triplicates are shown); at 1 nM Everolimus, a significant reduction of tumor cell numbers was observed for all NET/NEC human cell lines; however, even when using high concentrations (up to 10 µM), no complete tumor cell reduction could be achieved with Everolimus monotherapy. hpt, hours posttreatment; NEC, neuroendocrine carcinoma.

(Figure continued on next page.)

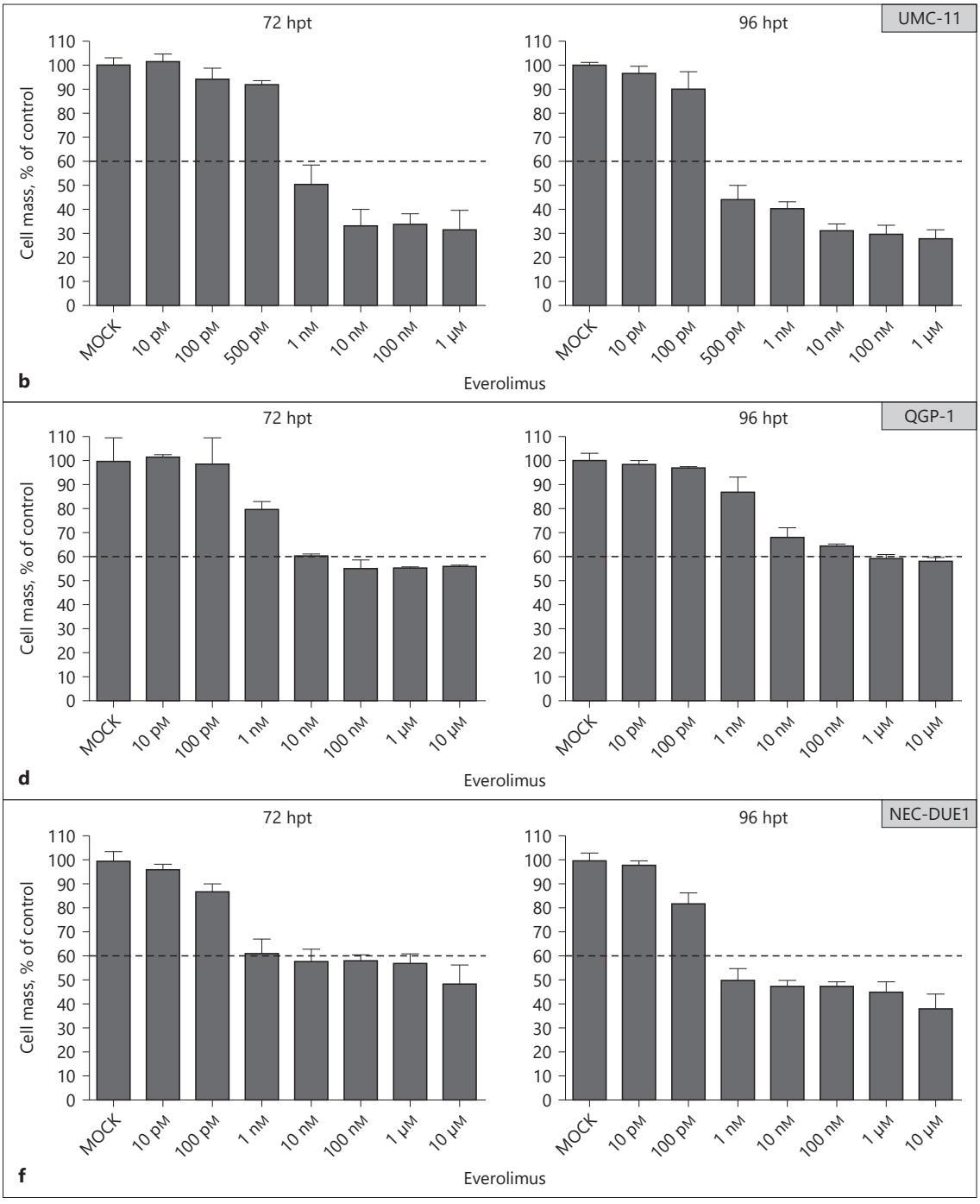

1

Transmission Electron Microscopy

The pNET cell line QGP-1 was infected with MOI 0.0001 and trypsinized and fixed in Karnovsky fixative after 24, 48, 72, and 96 h. For electron microscopic analyses, the cell pellets were embedded in 3.5% agarose at 37 °C, coagulated at room temperature, and fixed again in Karnovsky's solution. Postfixation was based on 1.0% osmium tetroxide containing 1.5% K-ferrocyanide in 0.1 M cacodylate buffer for 2 h. Samples were rinsed with distilled water, block-stained with uranyl acetate (2% in distilled water), dehydrated in alcohol (stepwise 30–96%), immersed in propylenoxide, embedded in glycide ether (polymerized 48 h at 60 °C, Serva, Heidelberg), and cut using an ultra microtome (Ultracut, Reichert, Vienna, Austria). Ultrathin sections (30 nm) were mounted on copper grids and analyzed using a Zeiss LIBRA 120 transmission electron microscope (Carl Zeiss, Oberkochen, Germany) operating at 120 kV.

Results

Everolimus Treatment

First, the antitumor potency of the FDA/EMA approved compound Everolimus was assessed via SRB viability assay on all 6 NET/NEC cell lines (Fig. 1). As a result, all cell lines showed a uniform response with a significant reduction of tumor cell numbers after 72 h when applying Everolimus concentrations of 1 nM and higher. Notably, lung NET cell line UMC-11 (Fig. 1b) was found to be most susceptible to Everolimus treatment, displaying a remnant cell number of only 45% after 96 h when applying Everolimus concentrations as low as 500 pM. Although all NET/NEC cell lines did respond quite well to Everolimus treatment, no complete reduction of tumor cell numbers (≤10%) could be achieved, even with concentrations up to 10 μM high. Residual tumor cell counts obtained at 96 h with the highest Everolimus concentrations were found to range between 60% (QGP-1; Fig. 1d) and 30% (UMC-11; Fig. 1b). These findings imply a search for potential combination partners not likewise belonging to molecular compounds, but may be to a different class of therapeutics such as biologicals, for example, virotherapeutics.

Virotherapy with T-VEC

In this context, our panel of NET/NEC human cell lines next was infected with the recombinant oncolytic HSV T-VEC, constituting a well-established virotherapeutic compound currently being under extensive clinical development. SRB assays were carried out in analogy to the Everolimus treatment to prove and compare cytostatic and cytotoxic/oncolytic effects. Then, the efficacy of a combinatorial treatment with both agents was assessed. Beyond that, viral titers also were determined sequentially to study and quantify replication of T-VEC in NET/NEC human tumor cells. Since T-VEC holds a GM-CSF cytokine transgene, also the amount of GM-CSF protein produced by T-VEC-infected NET/NEC cells was analyzed with an ELISA.

Oncolytic Cell Killing with T-VEC

For viability assays, tumor cells were infected with MOIs ranging from 0.0001 to 0.01. As a threshold for clinically relevant antitumor activities, 60% and less tumor cells being residual in SRB viability assays at 96 hpi was set for T-VEC (Fig. 2, dotted horizontal line). Based on the results of the SRB viability assays, MOIs had to be adjusted as follows: adding MOI 0.05 and 0.1 instead of MOI 0.0001 and 0.0005 for the QGP-1 and NEC-DUE1 cell line.

Infections with T-VEC resulted in a dose-dependent reduction of tumor cell numbers in all NET/NEC human cell lines (Fig. 2). Of note, T-VEC was found to mediate a highly efficient oncolysis in all NET/NEC cell lines, already at quite low MOIs. Four of six NET/NEC cell lines met the threshold of 60% tumor cells being residual at 96 hpi with the lowest MOI employed (0.0001). For QGP-1 cells, it took an MOI of 0.01. Interestingly, NEC-DUE-1 cells were identified to be relatively resistant to T-VEC oncolysis: no cytotoxicity was found after 72 h and only little cell killing could be observed after 96 h with the 2 highest MOIs employed (0.05 and 0.1). However, the 60% threshold could not be reached with this cell line (Fig. 2f). pNET cells BON-1 and lung NET cells UMC-11 were found to be most sensitive to T-VEC after 72 h, reaching a remaining cell count below 10% of mock with the highest MOIs (0.005 and 0.01). After 96 h, UMC-11 cells were found to be most susceptible to T-VEC-mediated tumor cell lyses, exhibiting a complete tumor cell reduction with all MOIs employed. Taken together, no completely resistant NET/NEC cell line could be detected at all.

In contrast, the highest MOI employed (0.1) resulted in a complete tumor cell count reduction in 5 of 6 NET/NEC cell lines at 96 hpi. Comparatively, treatment with Everolimus (Fig. 1) had not been able to reach such low residual tumor cell numbers at all.

Combinatorial Therapy

The results from monotherapy with either agent suggest a possible combinatorial therapy. Therefore, one cell line that was found to be susceptible to T-VEC treatment (H727) and the NEC-DUE1 cells, which were relatively resistant to T-VEC, were chosen and infected with MOI 0.00005 and MOI 0.1, respectively. Whereas monotherapy confirmed the results of the earlier experiments, the combinatorial treatment with T-VEC and Everolimus did not show a relevant additive effect (Fig. 3). In NEC-DUE1 cells, the combinatorial therapy turned out to be little more effective than Everolimus alone, but not in a relevant dimension. However, both agents seemed not to hamper each other and the remaining tumor cell count with the combinatorial therapy was found to be as high as the remaining cell count with the more effective (T-VEC in H727 cells and Everolimus in NEC-DUE1 cells) monotherapy.

Real-Time Cell Monitoring Assay

As the SRB viability assay displays a composite parameter of cytostatic and cytotoxic effects of the treatment

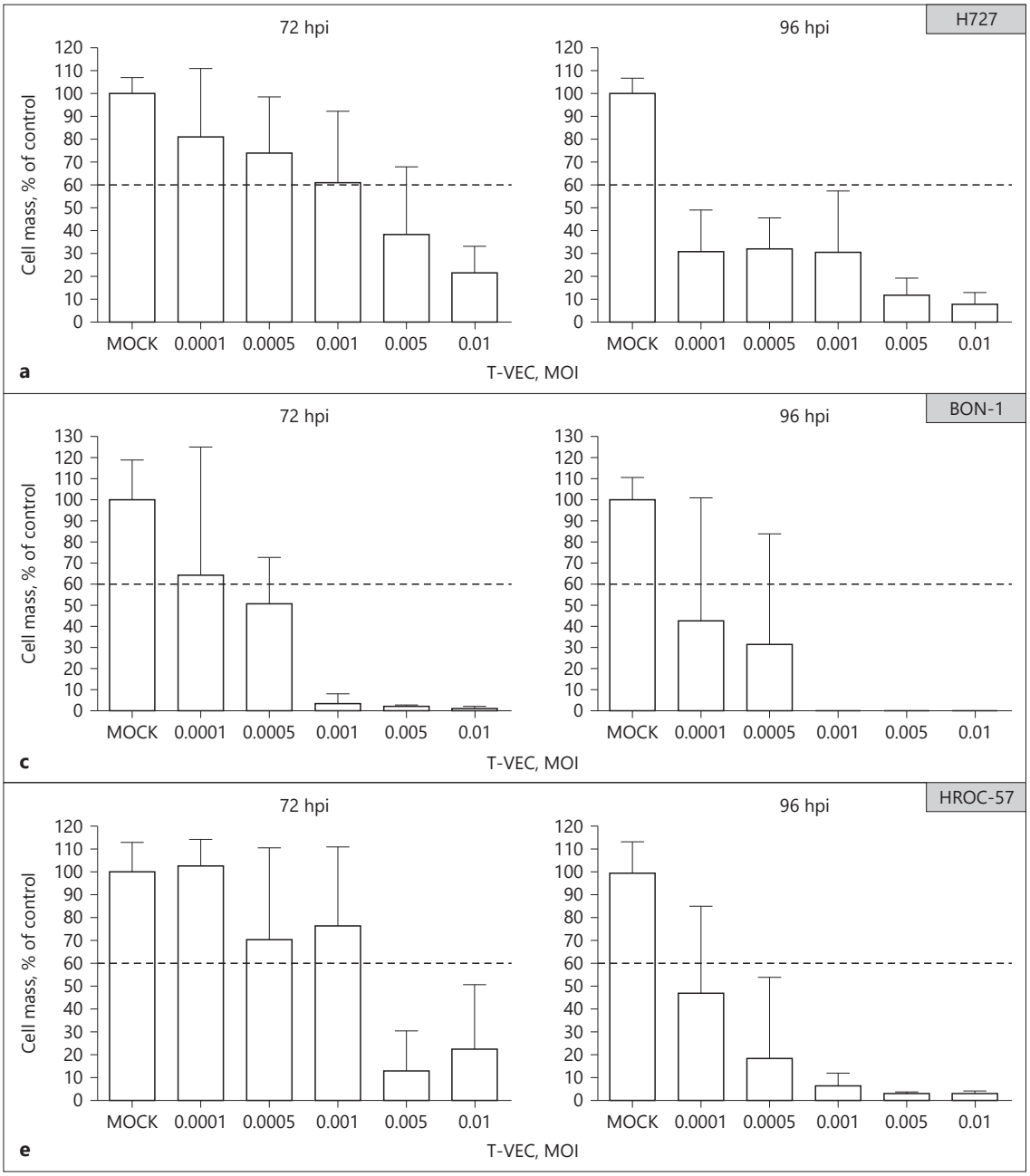

Fig. 2. SRB viability assays of the NET/NEC human tumor cell panel with recombinant HSV-1 derived virotherapeutic vector T-VEC (analysis performed at 72 and 96 hpi; mean and SD of 2 independent experiments carried out in quadruplicates are shown). T-VEC showed a highly effective cytoreduction already at extremely low MOIs; only in NEC-DUE1 cells, a relevant oncolytic effect could be observed only at 96 hpi when using much higher MOIs (up to 0.1). hpi, hours postinfection; T-VEC, talimogene laherparepvec; MOI, multiplicity of infection; NEC, neuroendocrine carcinoma.

(Figure continued on next page.)

agent employed, the cytotoxic nature of T-VEC was proved by continuous measurement of cell proliferation via real-time cell monitoring assay. In this purpose, the representative lung NET cell line H727 was used and treated with either T-VEC or Everolimus. As of 24 hpi (48 h on x-axis), T-VEC showed a dose-dependent reduction in cellular impedance, proving a cytotoxic effect (online suppl. Fig. S1; for all online suppl. material, see www.

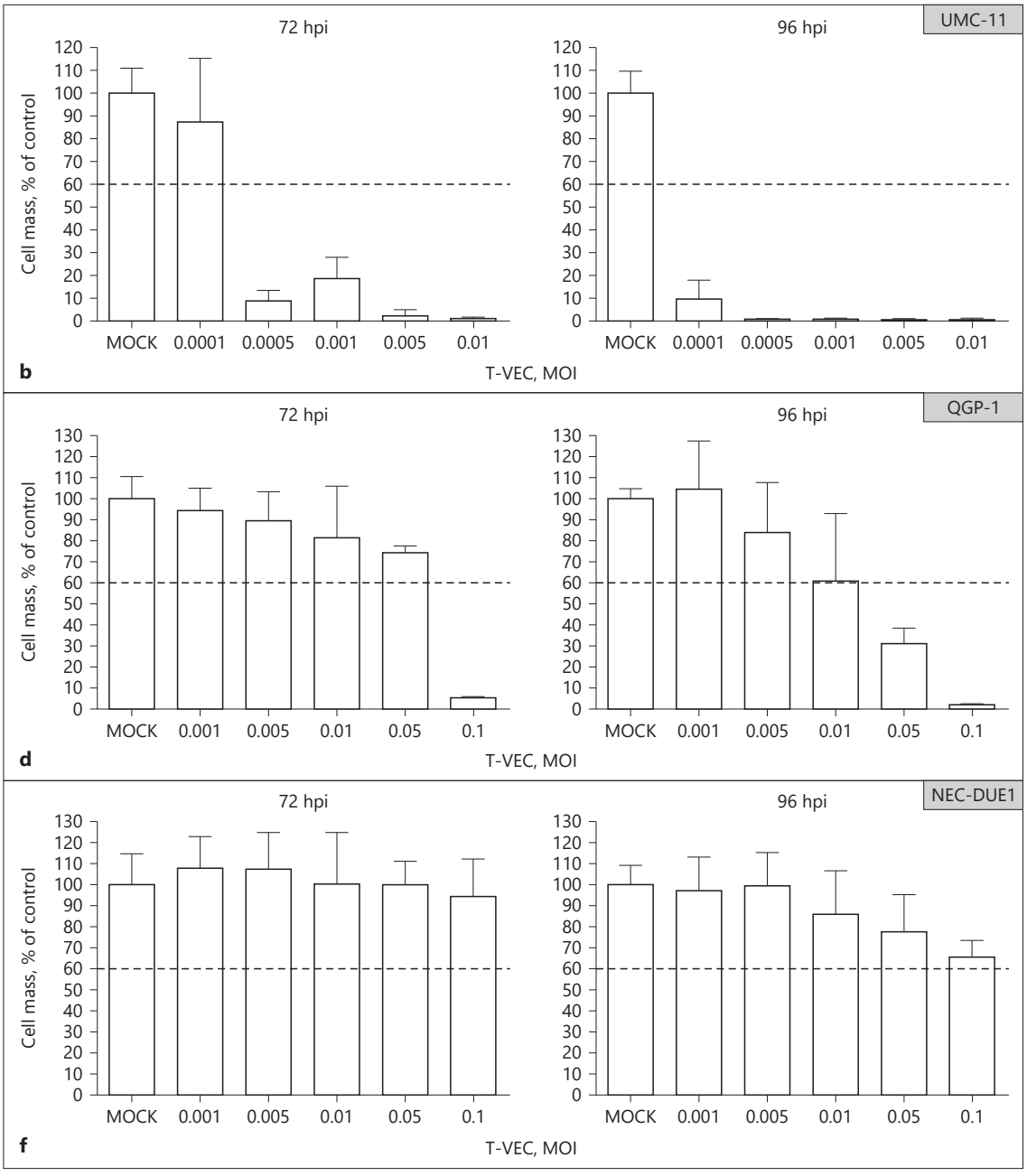

2

karger.com/doi/10.1159/000500159). On the other hand, Everolimus treatment only led to a slower cell proliferation (lower gradient of the curve) resulting in a reduced cell count compared to mock in SRB assay, although Everolimus was not able to reduce cell density over time (online suppl. Fig. S1). Concludingly, only a cytostatic effect of Everolimus could be observed, even with the high concentration of 100 nM.

Virus Replication of T-VEC

To measure virus replication of T-VEC in the absence and presence of Everolimus, 3 human NET/NEC cell lines from each anatomical origin were chosen (H727, QGP-1, NEC-DUE1). H727 cells were infected with MOI 0.0001; for QGP-1 and for NEC-DUE1 cells a MOI of 0.01 was employed, respectively. Of note, the lowest concentration of Everolimus that showed an effect in the previous viability assay (i.e., 1 nM) was picked for combinato-

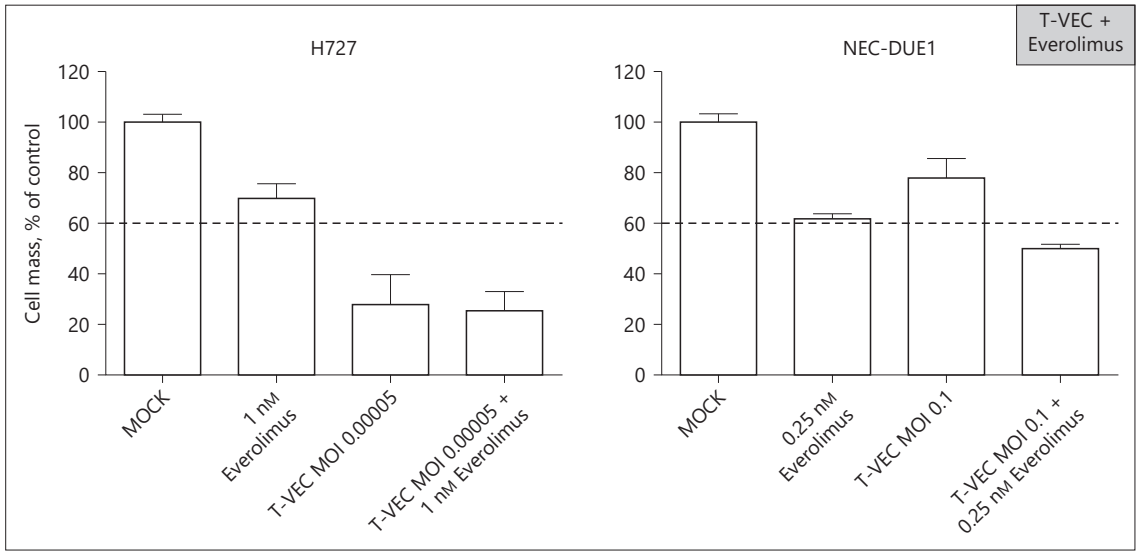

Fig. 3. SRB viability assays of 2 representative NET/NEC cell lines treated with Everolimus, T-VEC and the combination of both agents (analysis performed at 96 hpi/hpt; experiments were carried out in quadruplicates; bars show mean and SD). Although both agents exhibit significant effects in monotherapy, the combination therapy showed no relevant additive or synergistic effects. T-VEC, talimogene laherparepvec; MOI, multiplicity of infection; NEC, neuroendocrine carcinoma.

rial treatment (T-VEC + Everolimus). After infection, all free viral particles were removed so that only viral particles that had already entered the tumor cells could produce progeny.

With virotherapy alone, constantly growing virus titers were detected in all 3 cell lines and titers over 10^7 PFU/mL were reached (Fig. 4). The stagnation in virus titer growth after 72 h was explained by the efficient oncolytic depletion of tumor cells, resulting in significantly lower numbers of host cells being available for further rounds of infection and viral replication. This effect could be observed especially in H727 and QGP-1 cells (Fig. 4a, b) since both cell lines were found to be susceptible to oncolytic cell killing.

In NEC-DUE1 cells, slower but albeit still substantial replication kinetics of T-VEC were observed compared to the other cell lines, consistent with the results from the SRB viability assay, where NEC-DUE1 were identified to be the most resistant cell line. Nevertheless, T-VEC produced high virus titers also in NEC-DUE1 cells, indicating slow but sufficient virus replication and therefore a relative resistance to oncolysis.

Everolimus (1 nM) did only show small effects on viral titers; again, this difference can be explained by the lower number of host cells for viral replication resulting from an Everolimus-mediated cytotoxicity. In summary, no particular inhibitory effect of Everolimus on replication of T-VEC could be found.

Microscopy of T-VEC-Mediated NET/NEC Cell Oncolysis

Microscopic phase contrast pictures were also taken from T-VEC-infected human NET/NEC tumor cells at 72 hpi (online suppl. Fig. S2) and at 96 hpi (online suppl. Fig. S3), respectively. A major reduction in confluence of the tumor cell layers became visible in dependence of the MOI being applied (MOIs decrease from top to bottom), indicating T-VEC-mediated oncolysis, whereas mock treatment (pictures on top) always displayed the highest confluence.

T-VEC Encoded Transgene Expression

To prove expression of the T-VEC encoded GM-CSF transgene, an ELISA detecting human GM-CSF was employed. Two representative cell lines (H727 and NEC-DUE1) were first infected with T-VEC using MOI 0.0001 and MOI 0.1. Then supernatants were collected and analyzed every 24 h. At 1 hpi, no GM-CSF protein could be detected at all (Fig. 5). However, at 24 hpi, a low GM-CSF concentration of 128 pg/mL became detectable in H727 cell lines, whereas in NEC-DUE1 a slightly higher concentration of 163 pg/mL was measured. Then, GM-CSF con-

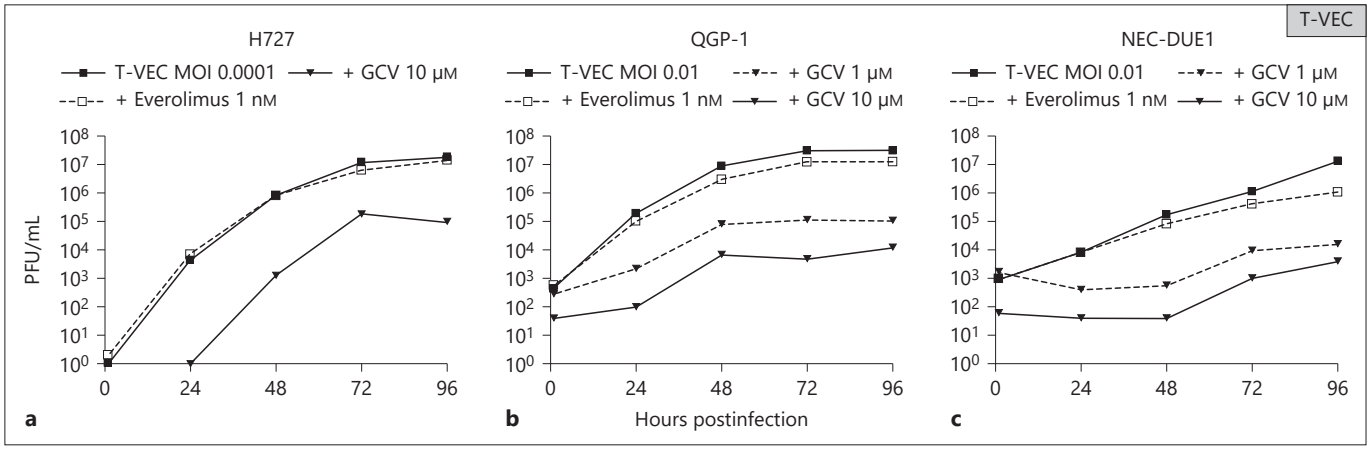

Fig. 4. Virus growth curves performed for virotherapeutic compound T-VEC in absence and presence of Everolimus or GCV, using representative NET/NEC cell lines H727 of lung origin, QGP-1 cells of pNET origin and NEC-DUE1 cells. GCV or Everolimus were added 1 hpi (**a**). PFU were determined every 24 h. Samples were analyzed in duplicates, experiments were performed twice, one representative result is shown. Employing H727 cells, T-VEC showed effective replication reaching virus titers over 10^6 PFU/mL at 48 hpi and maximum titers over 10^7 PFU/ml at 72 hpi (**a**, line dotted by black squares). Whereas Everolimus did not affect viral replication (**a**, line dotted by white squares), GCV (10 μM) was found to attenuate virus replication, lowering the maximum virus titer to 10^5 PFU/mL (**a**, line dotted by triangles). In QGP-1 pNET cells (**b**), T-VEC showed similar replication kinetics to H727 cells of lung origin, whereas viral replication was much slower in NEC-DUE1 cells (**c**), consistent with their relative oncolysis resistance shown in the SRB viability assay. Everolimus did not have any significant impact on viral replication (slightly lower virus titers being explained by the cytotoxicity being inherent to Everolimus, resulting in lower numbers of virus host cells). GCV attenuated viral replication in a dose dependent way in QGP-1 as well as in NEC-DUE1 cells. PFU, plaque forming unit; T-VEC, talimogene laherparepvec; MOI, multiplicity of infection; NEC, neuroendocrine carcinoma;. GCV, ganciclovir; hpi, hours postinfection.

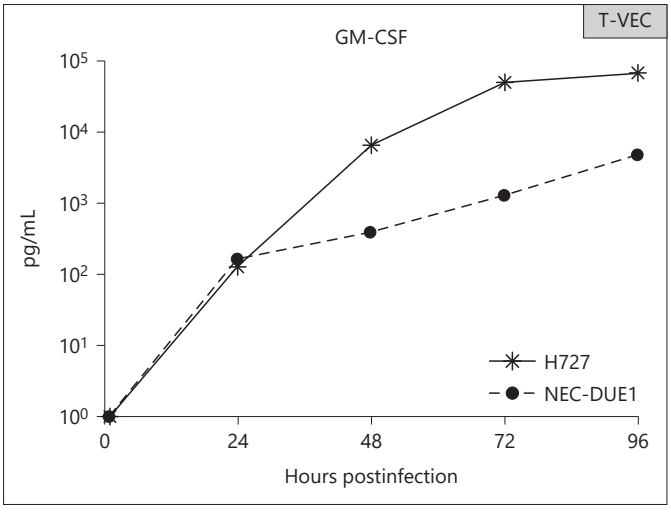

Fig. 5. Expression of the T-VEC encoded GM-CSF cytokine gene could be detected with an ELISA first at 24 hpi, reaching its highest level at 96 hpi in both cell lines. Of note, GM-CSF concentration increased more slowly in NEC-DUE1 cells, this can be explained by the limited replication of T-VEC in this cell line (Fig. 4). T-VEC, talimogene laherparepvec; NEC, neuroendocrine carcinoma.

centrations were found to increase constantly over time in both cell lines, finally reaching their maxima of 68 ng/mL at 96 hpi in H727 cells and of 4.7 ng/mL in NEC-DUE1 cells. Taken together, strong transgene expression could be proved in particular in H727 cells, again indicating a highly significant infection and replication of T-VEC in H727 tumor cells. Lower transgene expression was found in NEC-DUE1 cells indicating a correlation between virus replication and transgene expression, as T-VEC replication was shown to be limited in NEC-DUE1 cells.

GCV as a Safety Compound

The virostatic drug GCV was investigated for its ability to attenuate the replication of T-VEC in human NET/NEC cells. For this purpose, virus replication was analyzed after the addition of GCV in concentrations of 1 or 10 μM and compared to the replication in the absence of GCV. Again, NET/NEC cell lines H727, QGP-1, and NEC-DUE1 were infected, but now GCV was added at 1 hpi.

As a result, GCV was found to lower viral titers in all cell lines tested in a dose-dependent manner (Fig. 4). In H727 cells, 10 μM GCV reduced the maximum virus titer by log 2 PFU/mL, the first relevant increase in virus titer

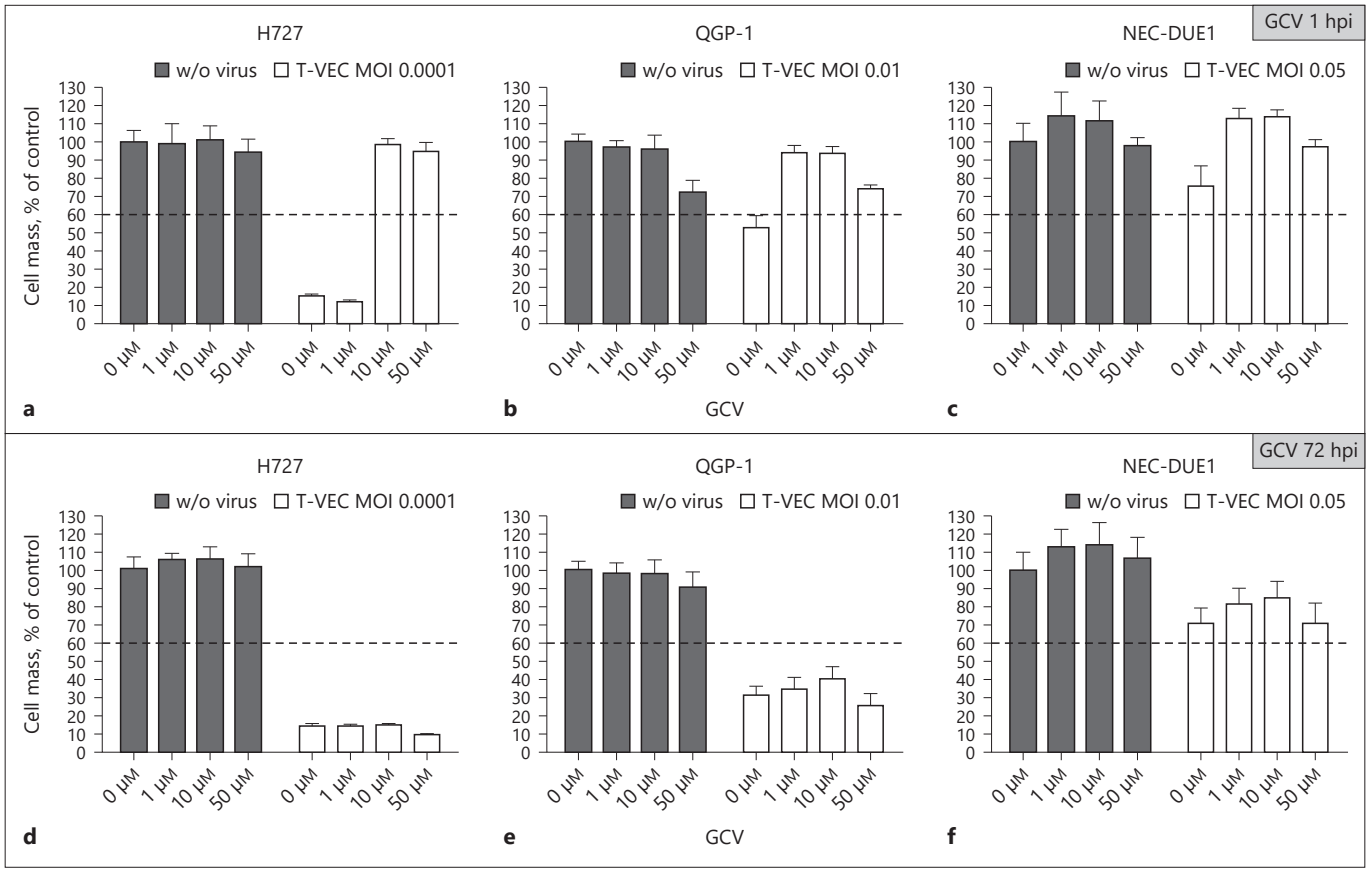

Fig. 6. GCV treatment of 3 T-VEC-infected NET cell lines (chosen from lung, pancreas, and upper gastrointestinal tract); SRB viability assays were performed at 96 hpi (mean and SD of 3 independent experiments carried out in triplicates are shown). When GCV was added at 1 hpi (**a**–**c**), 10 µM GCV were required to prevent T-VEC-mediated tumor cell killing in H727 cells (**a**); in contrast, 1 µM GCV was found to be sufficient in QGP-1 and NEC-DUE1 cells (**b**, **c**). Slight reductions in tumor cell counts obtained at 50 µM GCV are caused by the inherent cytotoxicity of GCV as they are similar in the T-VEC and mock treatment groups. When GCV was added as late as at 72 hpi (**d**–**f**), T-VEC-mediated tumor cell killing could not be completely ablated any longer; tumor cells already had been oncolysed to a large degree, thereby preventing expression of relevant amounts of HSV thymidine kinase (TK) being required for GCV's virostatic effects. With 50 µM GCV added at 72 hpi, again a small increase in cytotoxicity could be observed. hpi, hours postinfection; GCV, ganciclovir; T-VEC, talimogene laherparepvec; MOI, multiplicity of infection; NEC, neuroendocrine carcinoma.

was only detected after 48 h. In QGP-1 and NEC-DUE1 cells, 10 µM GCV reduced the highest virus titers by log 3 and 4, respectively. Taken together with the results from the viability assay, the efficacy of GCV was lower in highly susceptible cells (H727) and higher in more resistant cells (NEC-DUE1). More efficient and constant inhibition of viral replication possibly could be achieved by employing not only a single dose directly after viral infection but also repetitive doses of GCV.

To assess the impact of the GCV attenuated virus replication on oncolytic cell killing, viability assays were carried out with the addition of GCV at 1 and 72 hpi, employing GCV concentrations ranging from 1 to 50 µM (Fig. 6a–c). The same NET/NEC cell lines (H727, QGP-1, and NEC-DUE1) were tested as in the virus quantification experiment. When GCV was added at 1 hpi without virus, no toxicity could be observed in H727 cells, whereas little toxicity was detected in QGP-1 and NEC-DUE1 cells with 50 µM GCV. When the cells were infected with T-VEC using the respective MOIs, the results from the SRB viability assay were confirmed when no GCV was added (Fig. 6a–c, bars in black). Using GCV and T-VEC together, a complete inhibition of viral cytotoxicity could be observed with 10 µM GCV in H727 cells and with only 1 µM GCV in QGP-1 and NEC-DUE1 cells (Fig. 6a–c, bars in white). With 50 µM GCV, the reduction of rem-

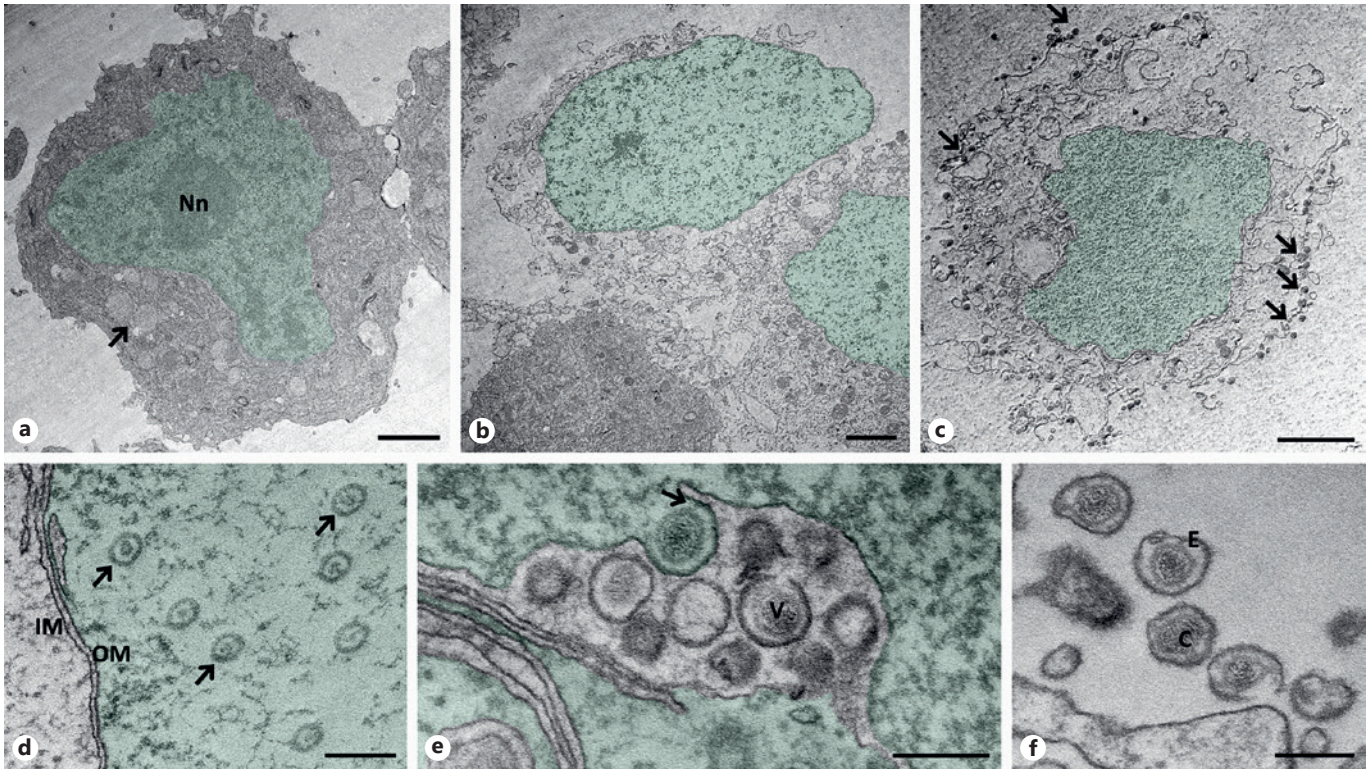

Fig. 7. Electron microscopic pictures of QGP-1 cells of pNET origin (nucleus green). Scale bars show 2 μm in (**a**–**c**) and 0.2 μm in (**d**–**f**). **a** Noninfected cell, nucleus (green) with a huge amount of euchromatin due to tumor cell characteristic synthesis and proliferative activity; electron dense nucleolus (Nn); secretory vesicles (single) being visible as QGP-1 cells secrete somatostatin, 5-HT as well as carcinoembryonic antigen. **b** T-VEC-infected cell (at 24 hpi; MOI 0.0001) exhibiting a nucleus containing almost only euchromatin (due to massive synthesis activity after T-VEC has occupied all cellular anabolic mechanisms required for production of huge amounts of progeny viral particles). **c** T-VEC oncolysed cell (at 96 hpi). The cell membrane now is completely covered with freshly produced virions (arrows). **d** Viral capsids (arrows) inside the nucleus with a diameter of approx. 100 nm. **e** Viral capsid budding at the IM (arrow). Enveloped capsids are detectable as complete virions (V) in the perinuclear space. **f** T-VEC virions with a size up to 200 nm in diameter consisting of a DNA containing nucleocapsid (C), tegument protein, and an envelope (E) with glycoprotein spikes. IM, inner nuclear membrane; OM, outer nuclear membrane.

nant tumor cell numbers was only due to the inherent cytotoxicity of GCV because presence/absence of T-VEC made no difference.

Furthermore, the virostatic effect of GCV was also studied by adding GCV as late as at 72 hpi, when viral replication and cell killing already were in full progress (Fig. 6d–f). In this setting, most of the tumor cells already had been lysed by T-VEC and GCV was found to limit the activity of T-VEC even after 72 h in QGP-1 and NEC-DUE1 cells (Fig. 6d–f, bars in white). With the addition of 10 μM GCV, 10–15% of the tumor cell population could be "saved." When GCV was added in a concentration of 50 μM, the inherent cytotoxicity of GCV outweighed and reduced the tumor cell count being residual at 96 hpi. In H727 cells, no relevant effect of GCV addition at 72 hpi could be detected, being consistent with the high susceptibility to T-VEC and the high virus titers despite GCV addition in this cell line.

In summary, GCV was not able to raise the remnant tumor cell numbers over the 60% threshold when it was added as late as 72 hpi. But GCV effectively prevented viral cytotoxicity when it was employed at 1 hpi although it did not completely bring down viral replication. Thereby, GCV can be regarded as an effective safety compound in the context of T-VEC mediated NET/NEC oncolysis.

Transmission Electron Microscopy

To visualize the viral egress and the envelopment of T-VEC, transmission electron microscopy (TEM) images

were taken from QGP-1 cells infected with MOI 0.0001 and compared with noninfected samples (Fig. 7). Beside direct identification of viral capsids or virions, also diverse morphological effects of T-VEC infections on QGP-1 cells of pNET origin could be demonstrated.

Compared to mock-infected QGP-1 cells (Fig. 7a), cells that were infected by T-VEC showed signs of massive protein and DNA synthesis, including a large amount of euchromatin in the nucleus, a dilated endoplasmic reticulum, and a swollen mitochondria. In a later stage of viral infection, T-VEC-mediated tumor cell lysis became visible, the cytoplasm lost its structure and the cell membrane was hardly detectable any longer (Fig. 7b). Whereas all these morphological changes could already be observed after 24 h, the first viral capsids and particles were detected after 72 h at first. This might be due to the low virus titers being applied (MOI 0.0001 "only") and therefore a small chance to cut viral particles at this early time point. In contrast, at 72 hpi, the tumor cells were completely surrounded by virions due to a massive synthesis of viral progeny particles (Fig. 7c).

The well-described pathways of wild-type HSV envelopment could be observed in a similar manner for the recombinant virotherapeutic derivative T-VEC (online suppl. Fig. S4). Briefly, viral capsids are produced in the nucleus (Fig. 7d), then bud at the inner nuclear membrane (IM) into the perinuclear space (Fig. 7e), or leave the nucleus via altered nuclear pores to bud at the outer nuclear membrane (OM), the endoplasmic reticulum or the Golgi network. Completed virions then get packaged into transport vacuoles to leave the cell and are released in the extracellular space by exocytosis (online suppl. Fig. S4). A third pathway of envelopment, including budding at the IM, deenvelopment at the OM, and secondary envelopment at cytosolic compartments, is described [29] but could not be retraced in this study. Taken together, when using TEM, recombinant T-VEC virions were found to be indistinguishable from wild-type HSV-1 virions, both containing a capsid, an envelope, and a tegument between, as visible structural components (Fig. 7f).

Discussion

T-VEC constitutes a state-of-the-art first-generation HSV-1-based OV exhibiting several favorable features, making it applicable for a broad spectrum of cancer entities. With its attenuating genetic modifications, it is not targeted to a specific type of tumor tissues but shows robust replication activity in neoplastic cells of several origins. The ICP 34.5 deletion ensures reduced neurovirulence and selective replication in cells with a defective protein kinase RNA-activated (PKR) signaling, a pathway which is dysregulated in many tumors. In healthy cells furnished with an intact PKR pathway, protein synthesis interrupts during virus infection mediated by an eIF-2a phosphorylation through PKR [30]. The innate cellular interferon response is another crucial feature for suppression of herpes virus infection and is also defective in many tumor cells [31]. A further advantage for T-VEC virotherapy is that this OV does not incorporate its viral DNA into the host genome, reducing the risk of virus induced mutagenesis. As demonstrated also in this work, there are multiple virostatic drugs such as GCV, acyclovir, or famciclovir, which exhibit an important safety feature for T-VEC based virotherapy. The problem of preexisting antibodies in the majority of the patient makes T-VEC unsuitable for systemic intravenous delivery. Nevertheless, it could be shown that preexisting antibodies reduce treatment related adverse events and viral shedding in case of intralesional virus delivery [8]. Hence, an initial lower dose of 10^6 PFU to induce seroconversion in seronegative patients has been incorporated in the regular treatment scheme [32], followed then by regular dosages of 10^8 PFU. For NET patients, intratumoral injections or infusions via the hepatic artery as already pursued by Yu et al. [13], employing an adenovirus-based recombinant virotherapeutic compound, also would be conceivable.

Until now, immunotherapy has not played a significant role in neuroendocrine cancer. There were approaches using dendritic cell vaccination [33] and a clinical phase I trial with an immune checkpoint inhibitor [34, 35], but results were not really encouraging. Recent studies show that only a small part of NETs and NECs show PD-L1 expression, which is the most encouraging target for immunotherapy so far [36]. But PD-L1 expression in metastatic NETs was found to be associated with higher WHO classification and worse overall survival [37]. The second well-established parameter for a response to immunotherapy is the tumor mutational burden, which is also relatively low in NETs [38]. Regarding the success of immune checkpoint inhibitors in non-SCLC and Merkel-cell carcinoma, these agents could possibly be efficient in similar tumors with a high tumor mutational burden like NECs [39]. Currently, clinical phase II/III studies investigating checkpoint inhibitors for treatment of neuroendocrine neoplasias are ongoing and are described in detail by Weber and Fottner [35]. Trials employing virotherapeutics, in particular adenoviral agents

and SVV, have been described above. In this context, oncolytic virotherapy might be a new way for immunotherapy to enter the field of neuroendocrine cancer.

In this paper, the ability of T-VEC to enter, replicate in, and lyse NET/NEC cells was demonstrated for the first time. Of note, high virus titers and high oncolytic activity of T-VEC were reached with strikingly low MOIs, underscoring the effectivity of viral replication in NET/NEC cells (Fig. 2). Interestingly, the cytotoxicity of T-VEC was found to be higher than in melanoma cell lines in a previous work [40]. In this paper, a MOI of 0.1 did not lead to a complete reduction of tumor cells after 72 h, in contrast to the results with most of the cell lines employed in this work. This capability was shown to be stable throughout cells derived from lung and pNETs and intestinal NECs. According to the preclinical nature of this study, any secondary, immune mediated antitumor effects could not be displayed when using our panel of NET/NEC human cell lines. However, this effect directly depends on the primary virus mediated oncolysis/cytotoxicity, which was presented here in a very convincing manner. In addition, high concentrations of the immunostimulatory GM-CSF transgene were detected, predicting a further increase in efficacy by immune effects in animal models and first human trials (Fig. 5). Interestingly, the curves showing virus replication and GM-CSF transgene expression seem to correlate in both cell lines tested (Fig. 4, 5). This proves that the inserted GM-CSF transgene is steadily expressed during virus replication in NET/NEC cell lines.

Combining T-VEC conducted virotherapy with other treatment modalities is a currently emerging strategy to improve response rates, especially in melanoma. In NETs, the targeted drugs Everolimus and Sunitinib are approved for treatment in advanced progressive stages, a situation where virotherapy could be a future option.

Since Everolimus is approved for a broader spectrum of neuroendocrine cancer, including progressive pNETs, intestinal NETs, and lung NETs, it was picked as aimed combinatorial treatment with T-VEC in this study. Furthermore, it is currently under clinical investigation for its efficacy in G3 NETs and NECs (NCT02113800). Given that background, the cytotoxic effects of T-VEC could be compared with an effective and widely approved drug in neuroendocrine cancer. T-VEC was found to reach a higher in vitro cytotoxicity than Everolimus in realistic dosing patterns, since tolerable Everolimus blood concentrations are known to reach up to 100 nM in peak and up to 20 nM over 24 h in patients [41]. Comparing the respective cytotoxicity at these concentrations in cell culture (Fig. 1) with the ones of T-VEC (Fig. 2), T-VEC was able to reach lower remnant tumor cell numbers with realistic MOIs. With Everolimus monotherapy, a stagnation of the treatment effect could be found with a dose of approximately 100 nM with most cell lines. As higher doses did not reach a significantly higher cytoreduction, a growth inhibitory rather than a cytotoxic effect of Everolimus could be assumed and proved with the real-time cell monitoring assay (online suppl. Fig. S1). In the context of synergistic effects of rapamycin (like Everolimus also belonging to the class of small molecule mTOR inhibitors) related and an oncolytic recombinant herpes virus, both agents seem to be possible combination partners for future NET/NEC treatment regimens [19]. In this work, no additive effects of a combinatorial therapy with T-VEC and Everolimus could be detected. The efficacy of the combination therapy was not found to be superior to the efficacy of the more effective monotherapy. Therefore, the effect of Everolimus on virus replication was assessed with the result that Everolimus was not found to alter/influence T-VEC replication (Fig. 4). Taken together, a combinatorial therapy with T-VEC and Everolimus is still arguable as the combination does not impair treatment efficacy, but whether combinatorial treatment can be more effective than monotherapy has to be further investigated.

In this context, the multikinase inhibitor Sunitinib could be another promising combination partner for T-VEC in treatment of neuroendocrine neoplasia. Sunitinib is approved for progressive pNET and was already shown to be a favorable combinatorial partner for virotherapeutics in a murine renal cell carcinoma model [42]. Moreover, it was found to augment antitumor properties of an oncolytic Vaccinia virus in a mouse model of progressive pNETs, underlining the potential of Sunitinib combined with an OV [43].

Interestingly, in terms of potential safety features, GCV was shown to significantly reduce virus replication (Fig. 4) and efficiently limit T-VEC-mediated cytotoxicity in NET/NEC cells (Fig. 6). A realistic tolerable blood concentration of GCV is approximately 5 μM in average over 24 h [44]. Regarding this, the experiments demonstrate that GCV is an applicable virostatic drug also in NET/NEC cells to ensure safety of T-VEC virotherapy in cases of any overwhelming virus replication scenarios which otherwise are unstoppable.

In a last step, both the viral egress and envelopment processes of T-VEC were visualized for the first time. The T-VEC virion has been observed under the TEM previously when it was investigated for its physical stability [45]. In this work, T-VEC capsid formation in the nucleus, budding at the IM, viral particles in the space between inner

and OM, and the transport for exocytosis were demonstrated in pNET cells (QGP-1, Fig. 7 and online suppl. Fig. S4). The 3 possible pathways of alphaherpesvirus envelopment have been described in detail earlier [46–48]. Whether deenvelopment at the OM and subsequent secondary envelopment at cytosolic compartments plays a role in T-VEC envelopment remains unclear. Morphological changes of the pNET cells were also detected. The massive formation of euchromatin shortly after virus infection indicates a lytic rather than a latent virus infection [49]. In summary, the efficient production and release of viral progeny could be observed, consistent with the fact of rapidly increasing virus titers in the other experiment (Fig. 4).

Taken together, this work suggests a highly promising perspective for T-VEC in the therapy of neuroendocrine cancers. Of note, this study constitutes only a first in vitro assessment including the well-known limitations in clinical predictability. However, it is expected to lay the foundation for future in vivo studies employing T-VEC in neuroendocrine cancers.

Acknowledgment

We are grateful to Amgen Inc., (Thousand Oaks, CA, USA) for providing T-VEC for our study.

Statement of Ethics

The authors have no ethical conflicts to disclose.

Disclosure Statement

The authors have no conflicts of interest to declare.

Funding Sources

L.D.K. is funded by the intramural *Interdisziplinäres Zentrum für Klinische Forschung* (Interdisciplinary Center for Clinical Research) scholarship of the Faculty of Medicine, University of Tübingen.

Author Contributions

L.D.K.: planned and performed the majority of the experiments and wrote the major part of the manuscript. S.B.: planned the experiments. I.S.: performed experiments. M.S. and B.F.: provided EM images. A.K.: established and provided NEC-DUE1 cells. B.S.: characterized the employed cell lines. U.M.L.: designed the study. All authors contributed to writing of the paper and read and approved the final manuscript.

References

1 Yao JC, Hassan M, Phan A, Dagohoy C, Leary C, Mares JE, et al. One hundred years after "carcinoid": epidemiology of and prognostic factors for neuroendocrine tumors in 35,825 cases in the United States. J Clin Oncol. 2008 Jun;26(18):3063–72.

2 Pavel M, O'Toole D, Costa F, Capdevila J, Gross D, Kianmanesh R, et al.; Vienna Consensus Conference participants. ENETS Consensus Guidelines Update for the Management of Distant Metastatic Disease of Intestinal, Pancreatic, Bronchial Neuroendocrine Neoplasms (NEN) and NEN of Unknown Primary Site. Neuroendocrinology. 2016; 103(2):172–85.

3 Schirrmacher V, Bihari AS, Stücker W, Sprenger T. Long-term remission of prostate cancer with extensive bone metastases upon immuno- and virotherapy: A case report. Oncol Lett. 2014 Dec;8(6):2403–6.

4 Dispenzieri A, Tong C, LaPlant B, Lacy MQ, Laumann K, Dingli D, et al. Phase I trial of systemic administration of Edmonston strain of measles virus genetically engineered to express the sodium iodide symporter in patients with recurrent or refractory multiple myeloma. Leukemia. 2017 Dec;31(12):2791–8.

5 Ribas A, Dummer R, Puzanov I, VanderWalde A, Andtbacka RH, Michielin O, et al. Oncolytic Virotherapy Promotes Intratumoral T Cell Infiltration and Improves Anti-PD-1 Immunotherapy. Cell. 2017 Sep;170(6):1109–1119.e10.

6 Marelli G, Howells A, Lemoine NR, Wang Y. Oncolytic Viral Therapy and the Immune System: A Double-Edged Sword Against Cancer. Front Immunol. 2018 Apr;9:866.

7 Hughes T, Coffin RS, Lilley CE, Ponce R, Kaufman HL. Critical analysis of an oncolytic herpesvirus encoding granulocyte-macrophage colony stimulating factor for the treatment of malignant melanoma. Oncolytic Virother. 2014 Jan;3:11–20.

8 Hu JC, Coffin RS, Davis CJ, Graham NJ, Groves N, Guest PJ, et al. A phase I study of OncoVEXGM-CSF, a second-generation oncolytic herpes simplex virus expressing granulocyte macrophage colony-stimulating factor. Clin Cancer Res. 2006 Nov 15;12(22): 6737–47.

9 Greig SL. Talimogene Laherparepvec: First Global Approval. Drugs. 2016 Jan;76(1):147–54.

10 Kaufman HL, Kim DW, DeRaffele G, Mitcham J, Coffin RS, Kim-Schulze S. Local and distant immunity induced by intralesional vaccination with an oncolytic herpes virus encoding GM-CSF in patients with stage IIIc and IV melanoma. Ann Surg Oncol. 2010 Mar;17(3):718–30.

11 Puzanov I, Milhem MM, Minor D, Hamid O, Li A, Chen L, et al. Talimogene Laherparepvec in Combination With Ipilimumab in Previously Untreated, Unresectable Stage IIIB-IV Melanoma. J Clin Oncol. 2016 Aug;34(22): 2619–26.

12 Rudin CM, Poirier JT, Senzer NN, Stephenson J Jr, Loesch D, Burroughs KD, et al. Phase I clinical study of Seneca Valley Virus (SVV-001), a replication-competent picornavirus, in advanced solid tumors with neuroendocrine features. Clin Cancer Res. 2011 Feb; 17(4):888–95.

13 Yu D, Leja-Jarblad J, Loskog A, Hellman P, Giandomenico V, Oberg K, et al. Preclinical Evaluation of AdVince, an Oncolytic Adenovirus Adapted for Treatment of Liver Metastases from Neuroendocrine Cancer. Neuroendocrinology. 2017;105(1):54–66.

14 Yamamoto Y, Nagasato M, Rin Y, Henmi M, Ino Y, Yachida S, et al. Strong antitumor efficacy of a pancreatic tumor-targeting oncolytic adenovirus for neuroendocrine tumors. Cancer Med. 2017 Oct;6(10):2385–97.
15 Essand M. Virotherapy of neuroendocrine tumors. Neuroendocrinology. 2013;97(1):26–34.
16 Jiao Y, Shi C, Edil BH, de Wilde RF, Klimstra DS, Maitra A, et al. DAXX/ATRX, MEN1, and mTOR pathway genes are frequently altered in pancreatic neuroendocrine tumors. Science. 2011 Mar;331(6021):1199–203.
17 Missiaglia E, Dalai I, Barbi S, Beghelli S, Falconi M, della Peruta M, et al. Pancreatic endocrine tumors: expression profiling evidences a role for AKT-mTOR pathway. J Clin Oncol. 2010 Jan;28(2):245–55.
18 Chan DL, Segelov E, Singh S. Everolimus in the management of metastatic neuroendocrine tumours. Therap Adv Gastroenterol. 2017 Jan;10(1):132–41.
19 Fu X, Tao L, Rivera A, Zhang X. Rapamycin enhances the activity of oncolytic herpes simplex virus against tumor cells that are resistant to virus replication. Int J Cancer. 2011 Sep; 129(6):1503–10.
20 Cheng PH, Lian S, Zhao R, Rao XM, McMasters KM, Zhou HS. Combination of autophagy inducer rapamycin and oncolytic adenovirus improves antitumor effect in cancer cells. Virol J. 2013 Sep;10(1):293.
21 Weng M, Gong W, Ma M, Chu B, Qin Y, Zhang M, et al. Targeting gallbladder cancer: oncolytic virotherapy with myxoma virus is enhanced by rapamycin in vitro and further improved by hyaluronan in vivo. Mol Cancer. 2014 Apr;13(1):82.
22 Linnebacher M, Maletzki C, Ostwald C, Klier U, Krohn M, Klar E, et al. Cryopreservation of human colorectal carcinomas prior to xenografting. BMC Cancer. 2010 Jul;10(1):362.
23 Kaku M, Nishiyama T, Yagawa K, Abe M. Establishment of a carcinoembryonic antigen-producing cell line from human pancreatic carcinoma. Gan. 1980 Oct;71(5):596–601.
24 Evers BM, Ishizuka J, Townsend CM Jr, Thompson JC. The human carcinoid cell line, BON. A model system for the study of carcinoid tumors. Ann N Y Acad Sci. 1994 Sep 15; 733:393–406.
25 Giaccone G, Battey J, Gazdar AF, Oie H, Draoui M, Moody TW. Neuromedin B is present in lung cancer cell lines. Cancer Res. 1992 May;52(9 Suppl):2732s–6s.
26 Krieg A, Mersch S, Boeck I, Dizdar L, Weihe E, Hilal Z, et al. New model for gastroenteropancreatic large-cell neuroendocrine carcinoma: establishment of two clinically relevant cell lines. PLoS One. 2014 Feb;9(2):e88713.
27 Takahashi T, Nau MM, Chiba I, Birrer MJ, Rosenberg RK, Vinocour M, et al. p53: a frequent target for genetic abnormalities in lung cancer. Science. 1989 Oct;246(4929):491–4.
28 Skehan P, Storeng R, Scudiero D, Monks A, McMahon J, Vistica D, et al. New colorimetric cytotoxicity assay for anticancer-drug screening. J Natl Cancer Inst. 1990 Jul;82(13):1107–12.
29 Johnson DC, Baines JD. Herpesviruses remodel host membranes for virus egress. Nat Rev Microbiol. 2011 May;9(5):382–94.
30 He B, Gross M, Roizman B. The gamma(1)34.5 protein of herpes simplex virus 1 complexes with protein phosphatase 1alpha to dephosphorylate the alpha subunit of the eukaryotic translation initiation factor 2 and preclude the shutoff of protein synthesis by double-stranded RNA-activated protein kinase. Proc Natl Acad Sci U S A. 1997 Feb 4; 94(3):843–8.
31 Paladino P, Mossman KL. Mechanisms employed by herpes simplex virus 1 to inhibit the interferon response. J Interferon Cytokine Res. 2009 Sep;29(9):599–607.
32 Senzer NN, Kaufman HL, Amatruda T, Nemunaitis M, Reid T, Daniels G, et al. Phase II clinical trial of a granulocyte-macrophage colony-stimulating factor-encoding, second-generation oncolytic herpesvirus in patients with unresectable metastatic melanoma. J Clin Oncol. 2009 Dec;27(34):5763–71.
33 Papewalis C, Wuttke M, Seissler J, Meyer Y, Kessler C, Jacobs B, et al. Dendritic cell vaccination with xenogenic polypeptide hormone induces tumor rejection in neuroendocrine cancer. Clin Cancer Res. 2008 Jul 1; 14(13):4298–305.
34 Patnaik A, Kang SP, Rasco D, Papadopoulos KP, Elassaiss-Schaap J, Beeram M, et al. Phase I Study of Pembrolizumab (MK-3475; Anti-PD-1 Monoclonal Antibody) in Patients with Advanced Solid Tumors. Clin Cancer Res. 2015 Oct;21(19):4286–93.
35 Weber MM, Fottner C. Immune Checkpoint Inhibitors in the Treatment of Patients with Neuroendocrine Neoplasia. Oncol Res Treat. 2018;41(5):306–12.
36 Sampedro-Núñez M, Serrano-Somavilla A, Adrados M, Cameselle-Teijeiro JM, Blanco-Carrera C, Cabezas-Agricola JM, et al. Analysis of expression of the PD-1/PD-L1 immune checkpoint system and its prognostic impact in gastroenteropancreatic neuroendocrine tumors. Sci Rep. 2018 Dec;8(1):17812.
37 Kim ST, Ha SY, Lee S, Ahn S, Lee J, Park SH, et al. The Impact of PD-L1 Expression in Patients with Metastatic GEP-NETs. J Cancer. 2016 Feb;7(5):484–9.
38 Lawrence MS, Stojanov P, Polak P, Kryukov GV, Cibulskis K, Sivachenko A, et al. Mutational heterogeneity in cancer and the search for new cancer-associated genes. Nature. 2013 Jul;499(7457):214–8.
39 Pavel ME, Sers C. WOMEN IN CANCER THEMATIC REVIEW: systemic therapies in neuroendocrine tumors and novel approaches toward personalized medicine. Endocr Relat Cancer. 2016 Nov;23(11):T135–54.
40 Liu BL, Robinson M, Han ZQ, Branston RH, English C, Reay P, et al. ICP34.5 deleted herpes simplex virus with enhanced oncolytic, immune stimulating, and anti-tumour properties. Gene Ther. 2003 Feb;10(4):292–303.
41 de Wit D, Schneider TC, Moes DJ, Roozen CF, den Hartigh J, Gelderblom H, et al. Everolimus pharmacokinetics and its exposure-toxicity relationship in patients with thyroid cancer. Cancer Chemother Pharmacol. 2016 Jul;78(1):63–71.
42 Lawson KA, Mostafa AA, Shi ZQ, Spurrell J, Chen W, Kawakami J, Gratton K, Thakur S, Morris DG. Repurposing Sunitinib with Oncolytic Reovirus as a Novel Immunotherapeutic Strategy for Renal Cell Carcinoma. Clin Cancer Res. 2016 Dec 1;22(23):5839–50.
43 Kim M, Nitschké M, Sennino B, Murer P, Schriver BJ, Bell A, et al. Amplification of Oncolytic Vaccinia Virus Widespread Tumor Cell Killing by Sunitinib through Multiple Mechanisms. Cancer Res. 2018 Feb;78(4): 922–37.
44 Lalezari JP, Friedberg DN, Bissett J, Giordano MF, Hardy WD, Drew WL, et al.; Roche Cooperative Oral Ganciclovir Study Group. High dose oral ganciclovir treatment for cytomegalovirus retinitis. J Clin Virol. 2002 Feb; 24(1–2):67–77.
45 Kumru OS, Joshi SB, Thapa P, Pheasey N, Bullock PS, Bashiri H, et al. Characterization of an oncolytic herpes simplex virus drug candidate. J Pharm Sci. 2015 Feb;104(2):485–94.
46 Roizman BK, Whitley RJ. Herpes simplex viruses. In: Knipe DM, Howley PM, editors. Fields virology. Philadelphia: Lippincott Williams & Wilkins; 2013. pp. 1823–97.
47 Owen DJ, Crump CM, Graham SC. Tegument Assembly and Secondary Envelopment of Alphaherpesviruses. Viruses. 2015 Sep; 7(9):5084–114.
48 Leuzinger H, Ziegler U, Schraner EM, Fraefel C, Glauser DL, Heid I, et al. Herpes simplex virus 1 envelopment follows two diverse pathways. J Virol. 2005 Oct;79(20):13047–59.
49 Knipe DM, Cliffe A. Chromatin control of herpes simplex virus lytic and latent infection. Nat Rev Microbiol. 2008 Mar;6(3):211–21.